Analysis of the wind field during the 'Vendée Globe' race: A kinematic SAR wind speed algorithm

V. Kerbaol, B. Chapron & P. Queffeulou

Laboratoire d'Océanographie Spatiale
Ifremer, France
e-mail: vkerbaol@ifremer.fr

A direct application of the recently derived SAR wind speed retrieval algorithm is presented in the particular case of the extremely high wind conditions endured by the competitors of the Vendée Globe sailing race between 7 and 8 January 1998. The wind speed analysis of a SAR ERS-2 wave-mode 'imagette' is presented to complete the measurements of other sensors (NSCAT, Topex and ERS-2 altimeter/scatterometer). In this area known as the 'Howling Fifties', the wind speeds during this period were extreme. Rapid veering conditions were as high as 23.6 m/s with the significant wave-height parameter estimated as high as 9 m.

Introduction

During the last Vendée Globe sailing race, extreme conditions were encountered by the competitors. Some had to abandon the race, and the presumed death of the Canadian sailor Gerry Roofs cast a tragic shadow over the event. His last known position was recorded on 7 January 1997 at - 55.01° S and 235.78° E (Fig. 1). Taking advantage of the different passes of various sensors over this area, we propose to analyse the wind and wave conditions as well as their evolution during this period.

The object of this study is to assess the wind speed as estimated from SAR images using a recently developed new algorithm based on the analysis of the SAR azimuth cut-off wavelength l_c. Such an algorithm is thought to be particularly successful during extremely high wind conditions while traditional wind retrieval algorithms based on the SAR backscatter measurements might be affected by saturation effects due to the analog-to-digital converter.

In the next section, the SAR wind speed algorithm (SWA) will be briefly presented. Then, the meteorological conditions will be described in light of the measurements of various sensors. Finally, the SWA will be applied on a collocated ERS-2 SAR wave-mode imagette.

Approximate route followed by the competitors of the Vendée Globe race (blue line). The last known position of Gerry Roofs is figured by a triangle.

①

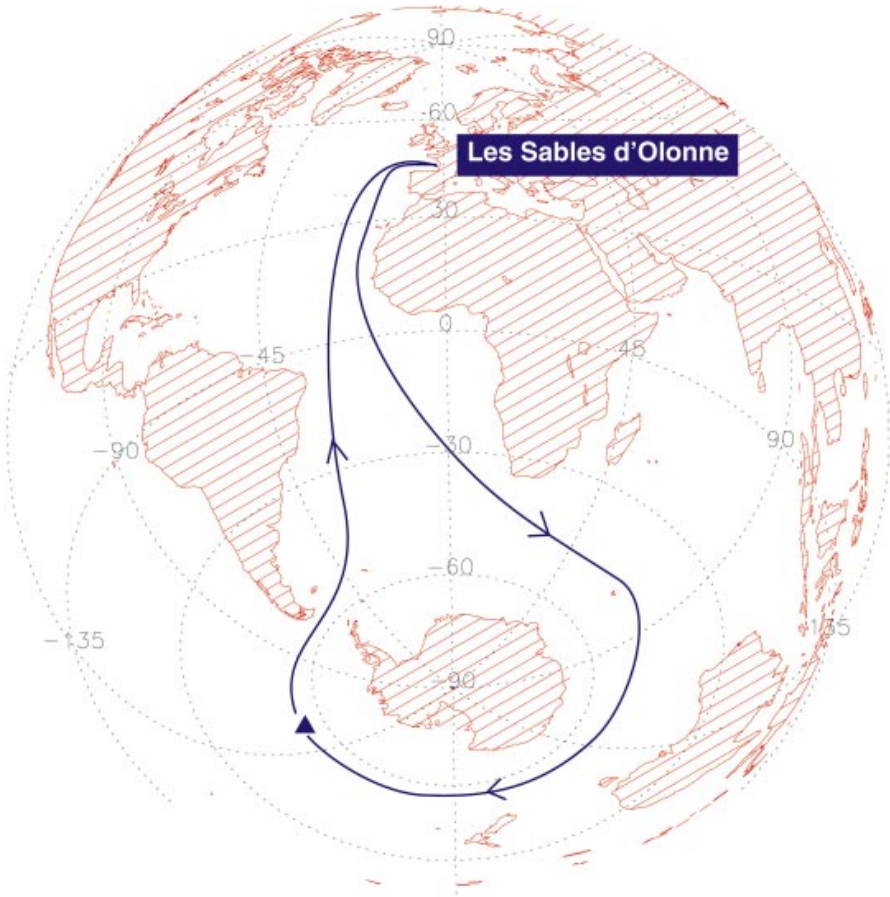

A new SAR wind speed algorithm
Known SAR Doppler mis-registrations in azimuth are induced by gravity-wave orbital motions, leading to a distortion of the imaged spectrum and a strong cut-off in the azimuthal direction. This effect is proportional to the range-to-platform velocity ratio *R/N*. ERS-1/2, Radarsat and future SAR missions, such as Envisat, are polar-orbiting platforms and have an *R/N* of about 120 s or larger. Then, depending on the sea-state, the shortest detectable wavelength in the azimuthal direction will not be less than 200 m.

At about 20° of incidence angle, orbital velocities components along a radar-target axis can be approximated to vertical components. The resulting SAR azimuth cut-off I_c is then directly bound to the standard deviation of azimuthal displacements and must be considered as a kinematic parameter accounting for vertical sea-surface motions occurring within the integration time. Consequently, it has proved to be a robust wind-driven sea-state indicator for ERS-1/2 SAR images. In particular, azimuth cut-off wavelengths estimated on SAR imagettes have been observed as a function of wind speed U_{10} inferred from collocated scatterometer measurements [*Kerbaol et al.* 1998]. Furthermore, it has been found that the cut-off value I_c can be empirically linearly related to the wind speed U_{10} as follows:

$$I_c = 23.5 \cdot U_{10} + 70 \qquad (1)$$

In addition, this simple algorithm has some particularly interesting properties, which make it especially useful in high wind conditions. First, the nearly exclusive dependency of the azimuth cut-off on vertical components of sea-surface orbital motions make this algorithm almost insensitive to the wave-propagation direction. Hence, the wind speed can be estimated without the *a priori* knowledge of wind/wave direction (such as given by meteorological model outputs or *in-situ* buoy measurements), which is essential when analysing the SAR backscatter signal [*Vachon & Dobson* 1996]. Moreover, the contribution of swell to the standard deviation of vertical components of orbital velocities, though not negligible under light wind conditions, is of minor importance in extremely high wind conditions [*Kerbaol et al.* 1998]. Thus, this wind speed estimation is not contaminated by residual sea-state independent of the local high wind conditions.

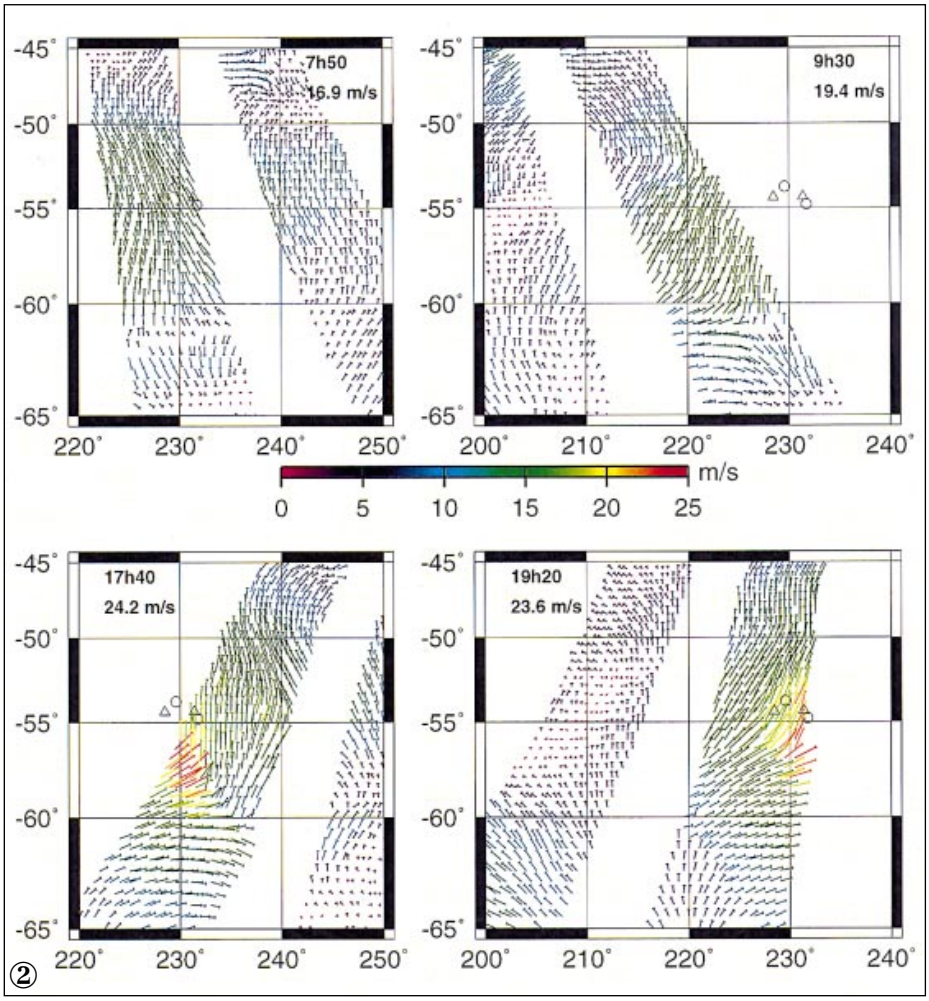

Wind field as estimated from NSCAT measurements on 7 Jan. 1998. G. Roofs's and I. Autissier's positions are represented respectively by circles and triangles.

Meteorological analysis
We now propose to analyse the meteorological situation on 7 January 1997 and its evolution up to the next day from the information given by different sensors passing over the area where G. Roofs last gave signs of life.

NSCAT Observations
Measurements of the American scatterometer NSCAT, acquired over the area of interest on 7 January (Fig. 2), show the rapid evolution of the wind field on that day in the proximity of the boats of G. Roofs (circles) and Isabelle Autissier (triangles). The wind vector variation in speed (from 16.9 to 23.6 m/s) as well as in direction (from about SE to SW) is likely to raise growing wave trains propagating at different directions, which are very difficult to negotiate. Note that the wind estimates merely represent a spatial average at a 50-km scale, while local gusts will likely be much stronger.

ERS-2/Topex altimeter measurements
The significant wave height (SWH) as estimated by ERS-2 and Topex altimeters on 8 January are presented (Fig. 3a). One observes that this

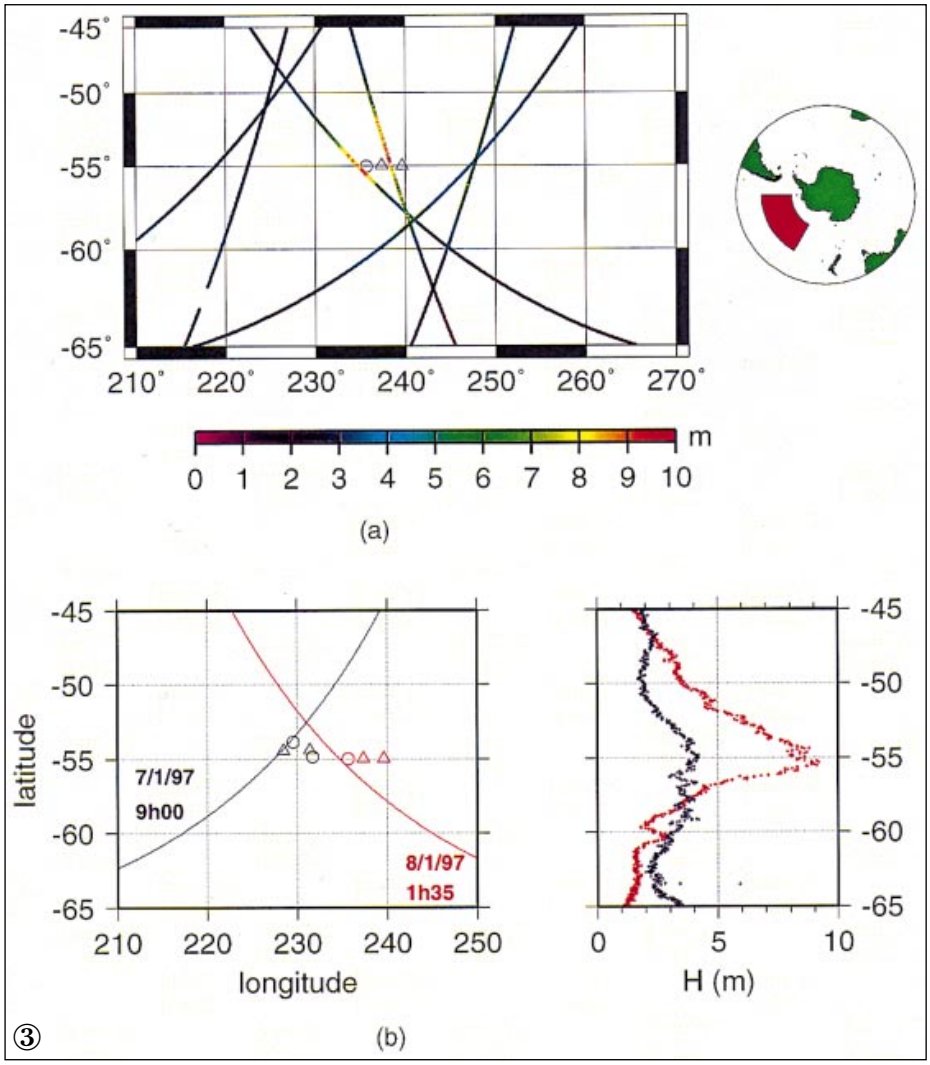

(a) Significant wave height estimates inferred from ERS-2 and Topex altimeter measurements on 8 Jan. (b) Evolution of the significant wave height as estimated from Topex measurements between 09:00 (7 Jan) and 01:35 (8 Jan). G. Roofs: circle; I. Autissier: triangle.

integrated parameter reaches values up to 9-10 m which means that individual waves are locally much higher. Moreover, a rapid wave growth occurs between 09:00 (7 Jan.) and 01:35 (8 Jan.) as captured by Topex measurements (Fig. 3b). Within only 18 h, SWH increased from 4 to 9 m.

ERS-2 SAR wind speed derived

On 8 January at 07:25, ERS-2 flew over this area; the related scatterometer swath is presented in Figure 4a. One can observe that the wind speed, inferred from scatterometer measurements using the empirical scattering model CMOD-Ifremer (Ifremer C2-MUT-W-01-IF), is as high as 17.8 m/s to the north-east of the recorded position of boats.

The ERS-1/2 band VV polarisation offers the unique opportunity to obtain interlaced scatterometer data and the so-called SAR wave mode imagettes (10 x 5 km). Thus, we extracted an imagette lying within the scatterometer swath (Fig. 4a). This sample image (Fig. 4b, left) as well as its 2D-oriented spectrum (right). Both the imaged long-crested features on the image itself and the strong compression of the spectral information along the range axis are characteristics of high winds which give, at first sight, an idea of the local extreme conditions.

An attempt was made to estimate the local wind speed from this imagette using our empirical wind speed retrieval algorithm based on the analysis of the SAR azimuth cut-off wavelength. The estimation of the cut-off value, simply obtained by fitting the Gaussian contribution of the detected modulation in the azimuthal domain of the auto-correlation function is presented in Figure 5. From this plot, the azimuth cut-off estimate is 559 m. Using our empirical linear relationship (eq. 1), the inferred wind speed is estimated to be as high as 20.9 m/s. Though not exactly of the same value, both scatterometer and SAR measurements are clearly consistent. Indeed, it is important to recall that the usual CMOD-type scattering model tends to underestimate the wind speed under high wind conditions.

Summary

The attempt was made to retrieve the wind speed from an ERS-2 SAR imagette using a SAR wind algorithm (SWA) based on the estimation of the SAR azimuth cut-off wavelength. Since SAR instruments are, in essence, sensitive to Doppler effects, the cut-off parameter is a good kinematic parameter representative of sea-surface vertical motions, which are predominantly driven by wind waves orbital velocities.

This study was highlighted by additional wind/waves field measurements as provided by Topex, NSCAT and ERS-2 scatterometer/altimeter. Though not unexpected in such an area known to be regularly swept by strong winds, the conditions were shown to be very extreme for sailing.

The agreement between our wind speed estimate and the wind speed traditionally estimated using backscatter power measurements suggests that this new algorithm will be quite accurate under high wind conditions. The non-dependency on any *a priori* information on wind direction is clearly another very interesting asset of our proposed use of the SAR azimuth cut-off parameter. In the near future, a combined analysis of

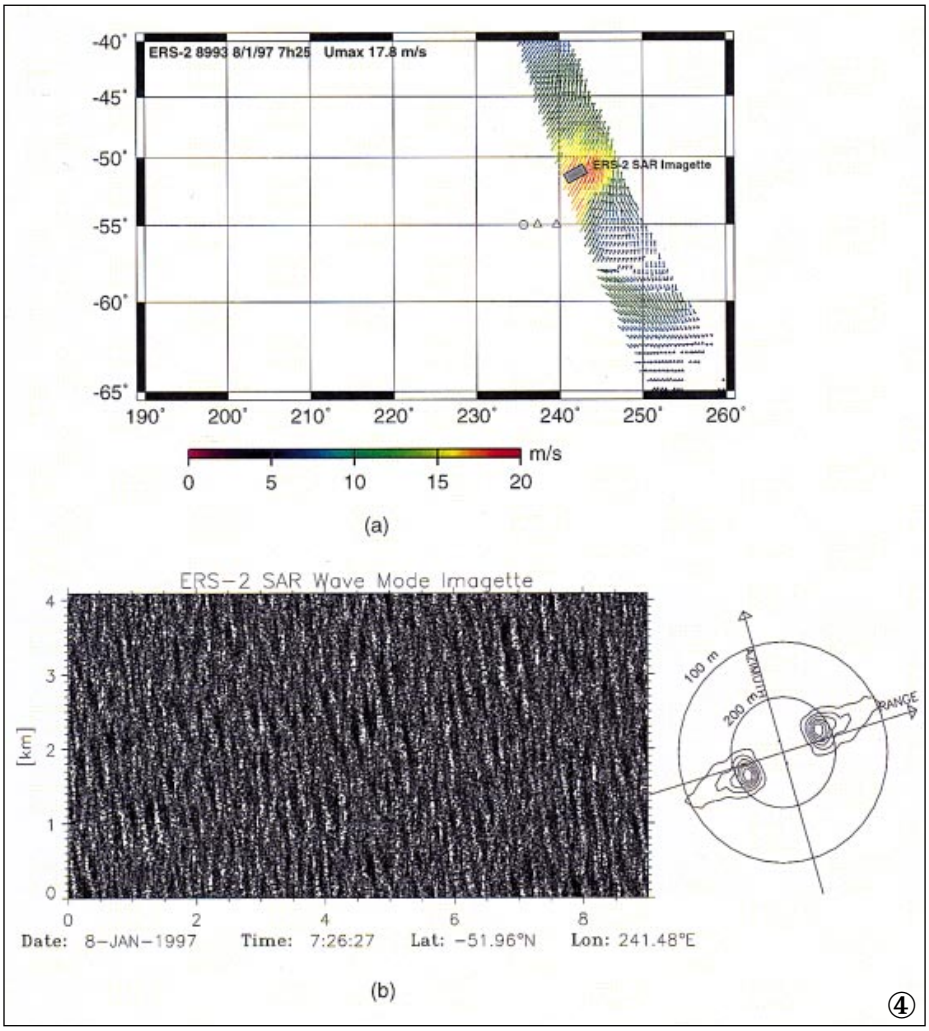

(a) ERS-2 scatterometer measurements of the 8 Jan. pass 07:25, showing G. Roofs's and I. Autissier's positions. (b) ERS-2 SAR wave mode imagette (left) and spectrum (right) lying within the scatterometer swath.

both azimuth cut-off and backscatter power should then help to refine the wind vector analysis from SAR images.

Analysis of the SAR azimuth cut-off wavelength estimated from ERS-2 SAR imagette (Fig.4b). The wind speed estimation using the SAR wind algorithm (eq. 1) is 20.9 m/s.

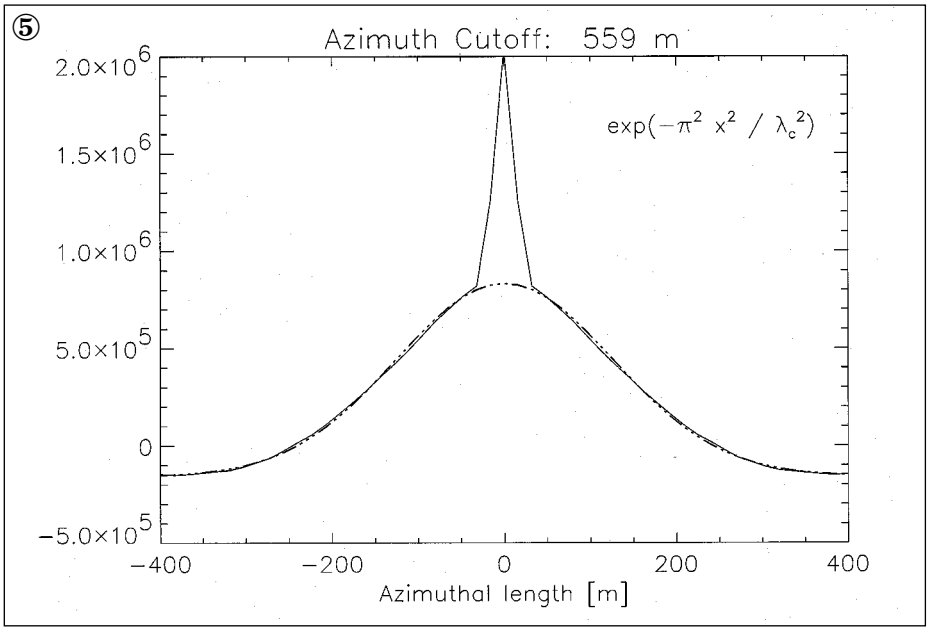

References

Ifremer C2-MUT-W-01-IF: Off-line wind scatterometer (ERS) products - User Manual (version 2.0), 1996.

Kerbaol V, B Chapron & PW Vachon: Analysis of ERS-1/2 SAR wave mode imagettes, *JGR* **103**, C4, 7833-7846,1998.

Vachon PW & FW Dobson: Validation of wind vector retrieval from ERS-1 SAR images over the ocean, *Global Atmos. Ocean Syst*. **5**,177-187.